

# Continuous wave single photon switch based on a Rydberg atom ensemble

Iason Tsiamis,<sup>1,2,\*</sup> Oleksandr Kyriienko,<sup>3</sup> and Anders S. Sørensen<sup>4</sup>

<sup>1</sup>*Dahlem Center for Complex Quantum Systems and Fachbereich Physik, Freie Universität Berlin, 14195 Berlin, Germany*

<sup>2</sup>*The Niels Bohr Institute, University of Copenhagen, Blegdamsvej 17, DK-2100 Copenhagen, Denmark*

<sup>3</sup>*Department of Physics and Astronomy, University of Exeter, Stocker Road, Exeter EX4 4QL, United Kingdom*

<sup>4</sup>*Center for Hybrid Quantum Networks (Hy-Q), The Niels Bohr Institute, University of Copenhagen, DK-2100 Copenhagen Ø, Denmark*

We propose an optical single-photon switch based on Rydberg atoms that interact through van der Waals interactions. A weak coherent field probes the atomic cloud continuously, and when a single photon excites a Rydberg state, it breaks the conditions for electromagnetically induced transparency, altering the reflection/transmission. Two versions of the device are proposed, one in a single-sided cavity and the other in free space. The proposed device extends the toolkit for quantum light manipulation and photon readout, and represents a continuous wave version of previously demonstrated single-photon transistors.

The rapid evolution of optical technologies demands efficient tools for controlling and modifying weak optical signals [1, 2]. Such tools typically rely on optical and microwave photons, which serve similar roles as electrical controls in conventional electronics. One such device is the optical quantum transistor, analogous to a classical field-effect transistor. Like its electronic counterpart, the optical quantum transistor uses a small optical control field to switch the propagation of another optical probe field on and off via nonlinear optical interaction. The fundamental limit of an optical quantum transistor is the single-photon transistor (SPT), where a single photon in the gate field controls the propagation of the weak coherent probe field.

Originally proposed for an atom coupled to a surface plasmon mode in a nanowire [3], the realization of a SPT requires a system with a large nonlinearity strongly coupled to individual photons. One promising candidate is a cloud of Rydberg atoms, which are strongly nonlinear due to their large van der Waals interaction [4]. Rydberg atoms have facilitated rapid progress in quantum optics and computing [5–7], allowing for the realization of strong photon-photon interactions [8, 9] and applications like Wigner crystallization [10], quantum gates [11–15], quantum simulation [16–21], and quantum optimization [22–24]. Several Rydberg-based coherent switches have been realized, promising optical control at the quantum level [25–28]. While similar SPTs have been demonstrated in other optical systems [29–32], they do not operate in the continuous wave (CW) regime required for applications. A CW SPT has been proposed in the microwave regime [33–37], but to the best of our knowledge no such device has been proposed to work in the optical regime.

In this Letter we propose and analyze a CW SPT based on an ensemble of driven Rydberg atoms, which can operate both in free space (FS) and inside a cav-

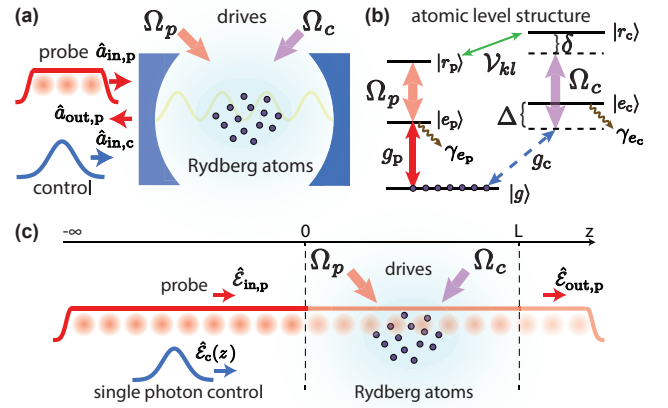


FIG. 1. (a) Sketch of the system, showing the cavity version of the Rydberg-based single photon transistor. (b) Atomic level scheme that illustrates multiple atomic states, which are divided into probe and control  $\Xi$ -systems. Each system is characterized by its own couplings and detunings. Additionally, the diagram shows the inter- $\Xi$ -system van der Waals interaction  $V_{kl}$ . (c) Free space device configuration, where the probe and control fields propagate inside the Rydberg cloud, which fills the space interval  $\{0, L\}$ .

ity (Fig. 1). In the absence of a control photon, the system is in the regime of electromagnetically induced transparency (EIT), allowing probe photons to propagate without loss [38, 39]. A single control photon can be efficiently converted into a collective Rydberg excitation, leading to interaction-induced blockade [40] and breaking the EIT condition. This allows for distinguishing the presence or absence of a single control photon by measuring the probe. We demonstrate that the dephasing of the control photons induced by the probe can be controlled, leading to long probing times and high gain

of the transistor. The proposed CW SPT could be used as an efficient optical single-photon detector with high signal-to-noise ratio [33]. The continuous wave operation greatly simplifies the protocol and expands the potential applications of the transistor.

*Cavity Model.*—We begin by considering a Rydberg cloud located in a single-sided cavity, where the photon fields interact with the atoms through the cavity field. The system is depicted in Fig. 1(a) and the multilevel structure of the atoms is shown in Fig. 1(b). The same level structure was considered for pulsed operation in Ref. [41]. The corresponding Hamiltonian consists of five parts:  $\hat{\mathcal{H}}_{\text{probe}}$ ,  $\hat{\mathcal{H}}_{\text{control}}$ ,  $\hat{\mathcal{H}}_{\text{Ryd}}$ ,  $\hat{\mathcal{H}}_{\text{input}}$ , and  $\hat{\mathcal{H}}_{\text{res}}$ .

The probe Hamiltonian  $\hat{\mathcal{H}}_{\text{probe}}$  reads

$$\hat{\mathcal{H}}_{\text{probe}} = - \sum_{l=1}^N \hbar(g_p \hat{a}_p \hat{\sigma}_{e_p g}^l + \Omega_p \hat{\sigma}_{r_p e_p}^l + \text{h.c.}), \quad (1)$$

where a cavity photon on the probing branch is described by the creation operator  $\hat{a}_p^\dagger$  and couples to the atoms with coupling constant  $g_p$ . The classical drive couples the  $|e_p\rangle \leftrightarrow |r_p\rangle$  levels with resonant Rabi frequency  $\Omega_p$ . The operators  $\hat{\sigma}_{mn}^l = |m\rangle\langle n|$  describe the transition of the  $l$ -th atom between states  $|m\rangle$  and  $|n\rangle$ , where  $\{m, n\} \in \{g, e_c, r_c, e_p, r_p\}$  and  $N$  is the total number of atoms in the ensemble. We have here performed the rotating wave approximation and consider an excitation regime corresponding to EIT conditions.

The Hamiltonian for the control branch in a rotating frame reads

$$\begin{aligned} \hat{\mathcal{H}}_{\text{control}} = & \sum_{l=1}^N \hbar[\Delta \hat{\sigma}_{e_c e_c}^l + \delta \hat{\sigma}_{r_c r_c}^l - (\Omega_c \hat{\sigma}_{r_c e_c}^l + \Omega_c^* \hat{\sigma}_{e_c r_c}^l) \\ & + (g_c \hat{a}_c \hat{\sigma}_{e_c g}^l + g_c^* \hat{a}_c^\dagger \hat{\sigma}_{g e_c}^l)], \end{aligned} \quad (2)$$

where we have introduced the detuning  $\Delta = \omega_{e_c g} - \omega_{1,c}$  and the two-photon detuning  $\delta = \Delta - (-\omega_{r_c e_c} + \omega_{2,c})$ . The atomic transition frequencies are defined as  $\omega_{e_c g} = \omega_{e_c} - \omega_g$ ,  $\omega_{r_c e_c} = \omega_{r_c} - \omega_{e_c}$  and  $\omega_{1,c}$  is the resonant frequency of the cavity, while  $\omega_{2,c}$  the classical drive frequency. The frequencies  $\omega_g$ ,  $\omega_{e_c}$ ,  $\omega_{r_c}$  correspond to the energies of states  $|g\rangle$ ,  $|e_c\rangle$ ,  $|r_c\rangle$ , respectively. The detunings are illustrated in Fig. 1(b). The cavity photon in the control branch is described by the creation operator  $\hat{a}_c^\dagger$ , which couples to each atom with strength  $g_c$ , and the classical drive for the upper transition has strength  $\Omega_c$ .

The SPT exploits the strong interaction between atoms in highly-excited Rydberg states. The interaction Hamiltonian for the ensemble reads

$$\hat{\mathcal{H}}_{\text{Ryd}} = \hbar \sum_{l=1}^N \sum_{\substack{k=1 \\ l \neq k}}^N \mathcal{V}_{kl} \hat{\sigma}_{r_p r_p}^l \otimes \hat{\sigma}_{r_c r_c}^k, \quad (3)$$

where we consider the levels  $|r_p\rangle$  and  $|r_c\rangle$  to interact through the van der Waals interaction  $\mathcal{V}_{kl} = C_6/\rho_{kl}^6$ ,

where  $\rho_{kl}$  denotes the distance between the atoms and  $C_6$  is an interaction coefficient [4]. We note that for the control branch we will only consider a single incident photon, whereas the probe branch can contain more photons. Nevertheless we only include interactions between Rydberg atoms in different branches. This is justified if e.g. the principal quantum number of the control branch is much larger than for the probe so that it has much larger dipole matrix elements.

Finally, we include the input/output of the system by adding the environment and reservoir Hamiltonians,  $\hat{\mathcal{H}}_{\text{input}} + \hat{\mathcal{H}}_{\text{res}}$  in the standard form [42, 43]. Given the Hamiltonian, we can write the equations of motion and calculate the ability of the system to store the control photons and manipulate the probe [44, 45]. In the following we consider the probe and control branches separately, assuming that the characteristic time scales for probing to be much faster than the time scale of control photon storage, i.e. that there is a large difference in the (EIT/Raman) bandwidth of the probe and control branches.

*Free space model.*—We also consider a FS version of the CW SPT device. The system is sketched in Fig. 1(c), and assumes propagation of both probe and control signals along the  $z$ -axis in the Rydberg medium of length  $L$ . The main ingredients for the scheme are same as in the cavity case, but the input and output are considered before and after the active medium. Furthermore in Hamiltonians given by Eqs. (1)-(2) the cavity photon creation operator  $\hat{a}_{p/c}^\dagger$  is replaced by the travelling electromagnetic field creation operator  $\hat{\mathcal{E}}_{p/c}^\dagger(z)$ . For brevity, we will describe the general function of the SPT applicable to both the cavity and the FS model in the following sections, while pointing out any differences that exist between them, where relevant.

*Probing.*—First, let us consider the left branch of the atomic level scheme, which is probed by the weak coherent state. The corresponding equations of motion can be derived from  $\hat{\mathcal{H}}_{\text{probe}} + \hat{\mathcal{H}}_{\text{Ryd}}$ . For the cavity case they are supplemented by the input-output relation  $\hat{a}_{\text{in},p} + \hat{a}_{\text{out},p} = \sqrt{2\kappa_p} \hat{a}_p$  [48], and for the free space case, by the Maxwell equation for light propagation in the medium. Furthermore, we include decay  $\gamma_{e_p}$  for the excited state  $|e_p\rangle$ , while the Rydberg states are considered to be long-lived. The dynamics in the EOMs of the probe branch are conditioned on the atomic state in the control branch through an effective two-photon detuning conditioned on the operators  $\hat{\sigma}_{r_c r_c}^k$ . In the absence of Rydberg excitations the standard EIT conditions are recovered [38], such that on resonance the reflection from the cavity (or the transmission through the medium for the FS) of the probe field goes to unity. On the other hand, if there is an atom in the Rydberg state in the right branch  $|r_c^k\rangle$ , it will be altered. This leads both to the measurable response of the SPT and an associated

dephasing of the state  $|r_c^k\rangle$ .

To describe this, we solve the system in the frequency domain for the cases when there is no Rydberg excitation (no control photon = reference) and when there is a stored control photon. We outline the derivation briefly here, and refer the interested reader to Ref. [46] for full details. Assuming a coherent field as an input and no Rydberg excitations, we find steady state solutions  $\alpha_p$  for the cavity ( $\mathcal{E}_p$  for the FS) of the form  $\hat{a}_p = \alpha_p + \delta\hat{a}_p$  ( $\hat{\mathcal{E}}_p = \bar{\mathcal{E}}_p + \delta\hat{\mathcal{E}}_p$ ), where  $\delta\hat{a}_p$  ( $\delta\hat{\mathcal{E}}_p$ ) represents quantum fluctuations around a shifted mode. We also apply a similar transformation for the atomic variables. Next, we subtract the reference from the solution with a Rydberg excitation, allowing us to describe only the Rydberg-associated processes. In this picture, the output in the absence of a control field is the vacuum state, and we only consider the relevant differential signal.

For the cavity case under these transformations, the Lindblad jump operators associated with the change in cavity reflection  $\hat{L}_{\kappa_p}$  and spontaneous emission of the  $l$ -th atom  $\hat{L}_{ge_p}^l$  read

$$\hat{L}_{\kappa_p} = -\sqrt{2\kappa_p} \sum_{k=1}^N \sqrt{\frac{2}{\kappa_p} \frac{C_{b,p}^k \alpha_{in,p} \hat{\sigma}_{r_c r_c}^k}{[1 + C_{b,p}^k]}}, \quad (4)$$

$$\hat{L}_{ge_p}^l = -\sum_{\substack{k=1 \\ k \neq l}}^N \sqrt{\frac{\gamma_{e_p}}{\kappa_p} \frac{i2g_p \alpha_{in,p} \hat{\sigma}_{r_c r_c}^k}{[\gamma_{e_p} - i|\Omega_p|^2/\mathcal{V}_{kl}][1 + C_{b,p}^k]}}, \quad (5)$$

where  $|\alpha_{in,p}|^2$  is the coherent input photon rate. Here we have introduced the blockaded cooperativity parameter of the  $k$ -th atom in the probe branch  $C_{b,p}^k = \sum_{l=1}^N C_{b1,p}^{k,l}$ , where  $C_{b1,p}^{k,l} = (|g_p|^2/\kappa_p)/(\gamma_{e_p} - i|\Omega_p|^2 \rho_{kl}^6/C_6)$  is the single atom blockaded cooperativity of the  $l$ -th atom, due to the excited  $k$ -th atom. The blockaded cooperativity corresponds to the cooperativity of all atoms located within the Rydberg blockade, apart from the excited  $k$ -th atom itself [11].

For the FS case under these transformations, the dephasing jump operators due to change in transmittance of the probe and spontaneous emission of the  $l$ -th atom are respectively [46]

$$\hat{L}_{d_p} = -i\sqrt{2\gamma_{e_p}} \alpha_{in,p} \sum_{\substack{k=1 \\ k \neq l}}^N \sum_{l=1}^N \hat{\sigma}_{r_c r_c}^k d_{b1,p}^{k,l} D_{b,p}^{k,l}, \quad (6)$$

$$\hat{L}_{ge_p}^l = -i\sqrt{\frac{\gamma_e}{d_{p1}}} \alpha_{in,p} \sum_{\substack{k=1 \\ k \neq l}}^N \hat{\sigma}_{r_c r_c}^k d_{b1,p}^{k,l} D_{b,p}^{k,l}, \quad (7)$$

where  $D_{b,p}^{k,l} = \sum_{l'=1}^l d_{b1,p}^{k,l'} e^{-\sum_{l''=l'}^{l'} d_{b1,p}^{k,l''}} - 1$  is the blockaded optical depth attenuation due to propagation of the probe in the atomic medium towards the  $l$ -th atom due to a Rydberg excitation of  $k$ -th atom. The blockaded optical depth of the  $l$ -th atom is defined as  $d_{b1,p}^{k,l} =$

$d_{p1} \gamma_{e_p}/(\gamma_{e_p} - i|\Omega_p|^2/\mathcal{V}_{kl})$ , where  $d_{p1} = |g_p|^2 L/(c\gamma_{e_p})$  is the single atom optical depth and  $c$  the speed of light in the medium. Using the operators in Eqs. (4)-(5) for the cavity [Eqs. (6)-(7) for the FS] and the equations of motion for the control branch, the full dynamics of the system can be accessed.

*Impedance matching.*—An essential ingredient for the SPT is impedance matching such that an incoming control photon is converted to a Rydberg excitation with near unity probability. To achieve this condition, the reflection (transmission) of the control photon must go to zero for the cavity (FS), and the losses through the intermediate excited state  $|e_c\rangle$  should be suppressed thus ensuring complete transfer to an atomic Rydberg excitation. The scattering dynamics of the control branch is highly sensitive to intensity  $|\alpha_{in,p}|^2$  of probing on the left branch, which according to Eqs. (4)-(5) for the cavity [(6)-(7) for the FS] induces a dephasing rate  $\gamma_r^k$  on the  $k$ -th atom in the right arm. We consider  $\gamma_r^k$  to be equal for all atoms for the analytical estimates.

The equations of motion for the control branch can be derived from  $\hat{\mathcal{H}}_{\text{control}}$  and Eqs. (4-5) for the cavity ((6-7) for the FS), with the effect of  $\hat{H}_{\text{Ryd}}$  being included in the dephasing rate  $\gamma_r$  under the previous transformations. We can thus adjust the probing strength  $|\alpha_{in,p}|^2$  to optimize impedance matching of the control photons. It is desirable to operate in the regime of large detuning  $\Delta/\gamma_{e_c} \gg (C_c + 1)$  for the cavity ( $\Delta/\gamma_{e_c} \gg 2d_c$  for FS) to achieve longer lifetime via localization [51, 52]. Here  $C_c$  is the total cavity cooperativity  $C_c = |g_c|^2 N/(\kappa_c \gamma_{e_c})$  and  $d_c = |g_c|^2 NL/(c\gamma_{e_c})$  the total optical depth of the control branch. Furthermore, we find that the absence of reflection can be achieved for a detuned control field,  $\delta = |\Omega_c|^2/\Delta$ , if the (probing induced) dephasing rate  $\gamma_r$  for the Rydberg state is equal to the output rate of the cavity  $\gamma_{\text{out}} = C_c \gamma_e |\Omega_c|^2/\Delta^2$  [54] (of the medium  $\gamma_{\text{out}} = d_c \gamma_e |\Omega_c|^2/(2\Delta^2)$  for the FS). Calculating the probability to find an atom in the Rydberg state we find it equal to  $(2C_c)^2/(1 + 2C_c)^2$  for the cavity case and to  $d_c/(2 + d_c) \exp(\frac{2d_c(d_c(-\gamma_{e_c}^2 d_c/\Delta^2) - 2) - 4}{(d_c + 2)^2})$  for the FS case, thus leading to near unity excitation transfer for the large cooperativity case,  $C_c \gg 1$  or for large optical depth in the FS case ( $d_c \gg 2$ ). We have numerically verified this analytical estimate for various ensemble geometries [46].

*Characterization of the SPT.*—To assess the performance of the single photon transistor, we use a wavefunction Monte Carlo (wfMC) method [47, 49] to simulate the system dynamics starting with a Gaussian control pulse containing a single photon. This approach provides insight into the number of emitted photons conditioned on the presence of Rydberg excitation and their distribution in real time [46]. The localization of Rydberg excitation resulting from probe photon scattering plays a critical role in the functioning of the SPT, as it reveals the location of the blockaded region. During storage dynamics,

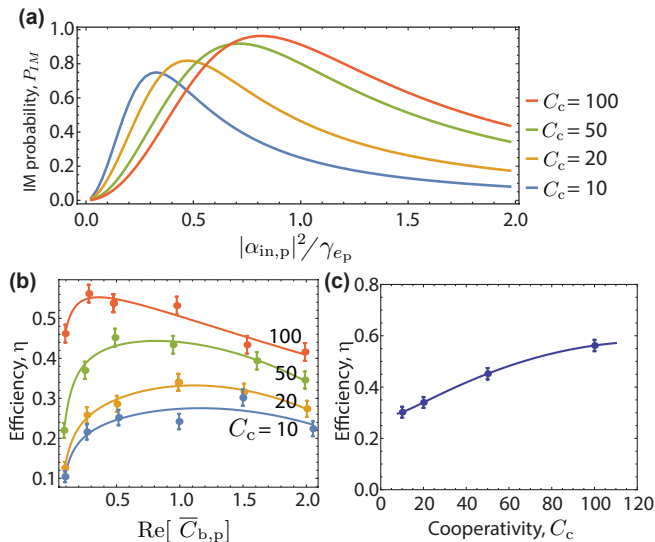


FIG. 2. Results of the cavity model with a 3D atomic ensemble of  $N = 10^3$  atoms randomly placed with an isotropic Gaussian distribution in 3D. The parameters for all plots are fixed to  $\Delta/\gamma_{ec} = 180$ ,  $\kappa_p/c = \gamma_{ep}/c$ ,  $\Omega_c/\gamma_{ec} = 5$ ,  $2\Omega_p/\gamma_{ec} = 10$ , and  $\delta$  varies between  $0.14\gamma_{ec}$  and  $0.1\gamma_{ec}$  to provide better IM. (a) Impedance matching probability as a function of probe strength for  $\text{Re}[\bar{C}_{b,p}] = 0.5$  and different values of the cooperativity  $C_c$ . (b) Efficiency of the SPT device as a function of blocked cooperativity. Solid curves show fitted polynomials and serve as a guide to the eye. (c) SPT efficiency as a function of cooperativity. At each point the blocked cooperativity and  $|\alpha_{in,p}|^2$  were optimized.

the excitation transfers to a collective superposition of  $|r_c\rangle$  coupled to a collective superposition of  $|e_c\rangle$ , which has an enhanced decay rate  $C_c\gamma_{ec}$  for the cavity ( $d_c\gamma_{ec}/2$  for the FS). This leads to an enhanced input/output rate  $\gamma_{out}$  by a factor of  $C_c \propto N$  ( $d_c/2 \propto N/2$ ). When the excitation localizes due to a spontaneous emission jump in the probe branch  $\hat{L}_{ge_p}^l$ , the number of atoms participating in the superposition decreases, resulting in a longer lifetime and enhanced gain of the transistor. However, this extended lifetime is only valid for large detuning i.e.  $\Delta \gg (C_c + 1)\gamma_{ec}$  for the cavity ( $\Delta \gg 2d_c\gamma_{ec}$  for FS), as on resonance, the lifetime becomes shorter due to localization [51–53]. Therefore, the proposed SPT can only function in the off-resonant regime, as previously studied in the context of spin wave decoherence [50].

To obtain the final readout of the SPT device, we can use either homo- or heterodyne detection to measure the output field difference resulting from the Rydberg blockade mechanism of the control photon. Another option is to use an interferometric setup, which cancels the probe signal on a photodetector when no control photons are present. Single photon detection of probe photons can then be used to detect the presence of a control photon,

which corresponds to a jump in the reflection (transmission) operator  $\hat{L}_{\kappa_p}$  ( $\hat{L}_{d_p}$ ) as described in Eq. (4) for the cavity (Eq. (6) for the FS) model. To evaluate the performance of the SPT device, we measure the number of such jumps and require it to be larger than a threshold number  $N_{\kappa_p/d_p}^{\text{th}} = 3$  for useful operation. The efficiency is defined as the probability of meeting this requirement. For homodyne detection, this threshold roughly corresponds to a signal squared that is six times the vacuum noise, but a precise assessment of the signal-to-noise ratio is complicated due to the multimode nature of the output field.

*Results for the cavity model.*—Our simulation uses an isotropic 3D Gaussian distribution of  $10^3$  randomly placed atoms. The system’s performance depends on the average blocked cooperativity  $\bar{C}_{b,p}$  and  $C_c$ . Although analytical description in this case is challenging, we obtained results using numerical wfMC calculations. Our results are presented in Fig. 2 and confirm that a large cooperativity is crucial in achieving a maximal IM probability, e.g. 0.963 for  $C_c = 100$ , in agreement with the analytically estimated IM conditions. Further details on the additional parameters used in the calculation can be found in the caption.

The SPT efficiency is presented in Fig. 2(b,c) and is found to be maximized at high cooperativities. A modest value of  $\bar{C}_{b,p} = 0.3$  and  $C_c = 100$  can yield a sizable efficiency of  $\eta \gtrsim 50\%$ . The storage lifetime of the control excitation determines the SPT gain, and it is enhanced by localization through spontaneous emission jumps. The optimal  $\bar{C}_{b,p}$  value depends on a trade-off between two factors: a small value favors the ratio of spontaneous emission jumps to cavity decay, while a not too small value facilitates signal readout through the cavity jump  $\hat{L}_{\kappa_p}$ . For a given  $\bar{C}_{b,p}$  value, a higher  $C_c$  is preferred for better impedance matching and localization after a jump. It is worth noting that our analysis does not involve a complete optimization of detuning  $\Delta$  and drive strengths  $\Omega_c$  and  $\Omega_p$ , so there may be room for further improvements. Current experiments have typical values of  $C_c$  of a few 10s [55, 56]. However, we expect future devices to achieve higher values.

*Results for the FS model.*— In the FS setup, we used a 1D Gaussian distribution of  $10^3$  randomly placed atoms over a distance  $L$ . Numerical wfMC calculations were conducted to obtain the results, as shown in Fig. 3. We verify the analytical IM estimate by numerically evaluating the impedance as a function of the intensity of the probe light which induces the dephasing, illustrated in Fig. 3(a). In contrast to the cavity case, the storage process in the FS protocol occurs in an exponentially decaying mode, due to the decreasing probability of an excitation propagating through the ensemble without being dephased. As a result, the readout Lindblad operator  $L_{d_p}$  also leads to localization, which enhances the lifetime of the stored control excitation. This means that the free

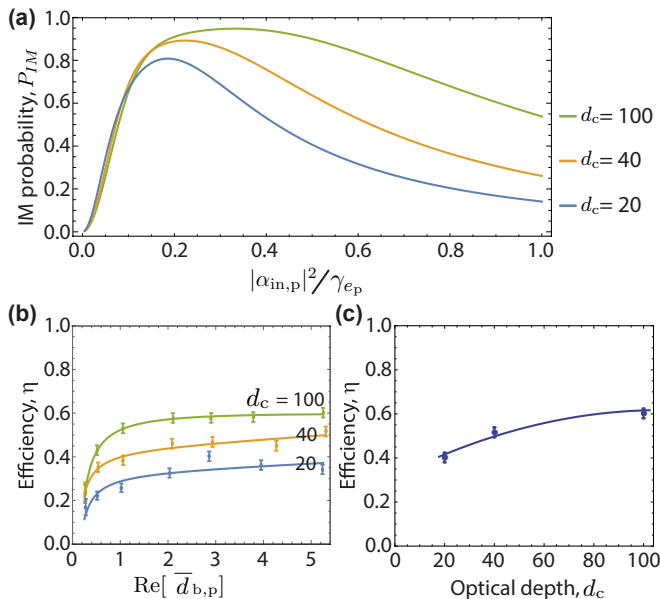


FIG. 3. Results for the free space model with a 1D atomic ensemble of  $N = 10^3$  atoms randomly placed with a Gaussian distribution in 1D. The parameters for all plots are fixed to  $\Delta/\gamma_{ec} = 2d_c$ ,  $\Omega_c/\Delta = 0.05$ ,  $\Omega_p/\gamma_{ec} = 10$ ,  $d_{1p/1c} = d_c/N$  and  $\delta/\gamma_{ec} = 0.113, 0.17, 0.45$  for  $d_c = 20, 40, 100$ . (a) Impedance matching probability as a function of probe strength with a blocked optical depth  $\bar{d}_{b,p} = 2$  and different optical depth  $d_c$ . (b) Efficiency of the SPT device as a function of average blocked optical depth. Solid curves show fitted polynomials and serve as a guide to the eye. (c) SPT efficiency as a function of optical depth. At each point the blocked optical depth and  $|\alpha_{in,p}|^2$  were fixed to be optimal.

space protocol can be operated with  $\bar{d}_{b,p} \gg 1$  (Fig. 3(b)), allowing for a larger change in the probe transmission compared to the cavity case where we required  $\bar{C}_{b,p} \lesssim 1$ . The maximal observed efficiency exceeds 60%, for  $d_c=100$  and  $\bar{d}_{b,p} = 5.3$ , as shown in Fig. 3(c). We note, however, that the choice of  $\bar{d}_{b,p}$  is not optimal, as it can be increased. It is important to also note that the operating conditions for the FS model were inspired by the cavity, and a full optimization was not conducted.

*Conclusions.*—We have proposed and analyzed an optical single photon transistor which can operate in the continuous wave regime, for an ensemble of Rydberg atoms both in a cavity and in free space. The estimated efficiency reaches 60% for the chosen (conservative) parameters. Currently our numerical simulation does not allow us to go to higher atom numbers, but the efficiency grows with ensemble size. We thus believe that even better efficiencies can be reached. The proposed device may thus open a new regime of continuous time control and manipulation of light with single photon fields in future devices.

*Acknowledgments.*—This work was supported by the ERC grant QIOS (Grant No. 306576). I.T. acknowl-

edges funding by the Deutsche Forschungsgemeinschaft through the Emmy Noether program (Grant No. ME 4863/1-1). A.S. acknowledges the support of Danmarks Grundforskningsfond (DNRF 139, Hy-Q Center for Hybrid Quantum Networks). O.K. acknowledges the support from EPSRC grants EP/V00171X/1 and EP/X017222/1, and NATO SPS project MYP.G5860.

\* [iason.tsiamis@fu-berlin.de](mailto:iason.tsiamis@fu-berlin.de)

- [1] H. J. Kimble, The quantum internet, *Nature (London)* **453**, 1023 (2008).
- [2] D. E. Chang, V. Vuletić, and M. D. Lukin, Quantum nonlinear optics – photon by photon, *Nat. Photon.* **8**, 685–694 (2014).
- [3] D. E. Chang, A. S. Sørensen, E. A. Demler, and M. D. Lukin, A single-photon transistor using nanoscale surface plasmons, *Nat. Phys.* **3**, 807 (2007).
- [4] M. Saffman, T. G. Walker, and K. Mølmer, Quantum information with Rydberg atoms, *Rev. Mod. Phys.* **82**, 2313 (2010).
- [5] A. Browaeys and T. Lahaye, Many-body physics with individually controlled Rydberg atoms, *Nat. Phys.* **16**, 132 (2020).
- [6] C. S. Adams, J. D. Pritchard, and J. P. Shaffer, Rydberg atom quantum technologies, *J. Phys. B* **53**, 012002 (2020).
- [7] L. Henriët, L. Beguin, A. Signoles, T. Lahaye, A. Browaeys, G.-O. Reymond, and C. Jurczak, Quantum computing with neutral atoms, *Quantum* **4**, 327 (2020).
- [8] O. Firstenberg, T. Peyronel, Qi-Yu Liang, A. V. Gorshkov, M. D. Lukin, and V. Vuletić, Attractive photons in a quantum nonlinear medium, *Nature (London)* **502**, 71 (2013).
- [9] A. V. Gorshkov, J. Otterbach, M. Fleischhauer, T. Pohl, and M. D. Lukin, Photon-Photon Interactions via Rydberg Blockade, *Phys. Rev. Lett.* **107**, 133602 (2011).
- [10] J. Otterbach, M. Moos, D. Muth, and M. Fleischhauer, Wigner Crystallization of Single Photons in Cold Rydberg Ensembles, *Phys. Rev. Lett.* **111**, 113001 (2013).
- [11] S. Das, A. Grankin, I. Iakoupov, E. Brion, J. Borregaard, R. Boddeda, I. Usmani, A. Ourjoumtsev, P. Grangier, and A. S. Sørensen, Photonic controlled-phase gates through Rydberg blockade in optical cavities, *Phys. Rev. A* **93**, 040303(R) (2016).
- [12] G. Higgins, F. Pokorny, Chi Zhang, Q. Bodart, and M. Hennrich, Coherent Control of a Single Trapped Rydberg Ion, *Phys. Rev. Lett.* **119**, 220501 (2017).
- [13] H. Levine, A. Keesling, G. Semeghini, A. Omran, T. T. Wang, S. Ebadi, H. Bernien, M. Greiner, V. Vuletić, H. Pichler, and M. D. Lukin, Parallel Implementation of High-Fidelity Multiqubit Gates with Neutral Atoms, *Phys. Rev. Lett.* **123**, 170503 (2019).
- [14] K. McDonnell, L. F. Keary and J. D. Pritchard, Demonstration of a Quantum Gate using Electromagnetically Induced Transparency, *Phys. Rev. Lett.* **129**, 200501 (2022).
- [15] D. Bluvstein, H. Levine, G. Semeghini, T. T. Wang, S. Ebadi, M. Kalinowski, A. Keesling, N. Maskara, H. Pichler, M. Greiner, V. Vuletić, and M. D. Lukin, A quantum

- processor based on coherent transport of entangled atom arrays, *Nature (London)* **604**, 451 (2022).
- [16] H. Labuhn, D. Barredo, S. Ravets, S. de Leseleuc, T. Macrì, T. Lahaye, and A. Browaeys, Tunable two-dimensional arrays of single Rydberg atoms for realizing quantum Ising models, *Nature (London)* **534**, 667 (2016).
- [17] H. Bernien, S. Schwartz, A. Keesling, H. Levine, A. Omran, H. Pichler, S. Choi, A. S. Zibrov, M. Endres, M. Greiner, V. Vuletić, and M. D. Lukin, Probing many-body dynamics on a 51-atom quantum simulator, *Nature (London)* **551**, 579 (2017).
- [18] M. Sbroscia, K. Viebahn, E. Carter, Jr-Chiun Yu, A. Gaunt, and U. Schneider, Observing Localization in a 2D Quasicrystalline Optical Lattice, *Phys. Rev. Lett.* **125**, 200604 (2020).
- [19] S. Ebadi, T. T. Wang, H. Levine, A. Keesling, G. Semeghini, A. Omran, D. Bluvstein, R. Samajdar, H. Pichler, Wen Wei Ho, Soonwon Choi, S. Sachdev, M. Greiner, V. Vuletic, and M. D. Lukin, Quantum phases of matter on a 256-atom programmable quantum simulator, *Nature (London)* **595**, 227 (2021).
- [20] G. Semeghini, H. Levine, A. Keesling, S. Ebadi, T. T. Wang, D. Bluvstein, R. Verresen, H. Pichler, M. Kalinowski, R. Samajdar, A. Omran, S. Sachdev, A. Vishwanath, M. Greiner, V. Vuletic, and M. D. Lukin, Probing Topological Spin Liquids on a Programmable Quantum Simulator, *Science* **374**, 1242 (2021).
- [21] A. J. Daley, I. Bloch, C. Kokail, S. Flannigan, N. Pearson, M. Troyer, and P. Zoller, Practical quantum advantage in quantum simulation, *Nature (London)* **607**, 667 (2022).
- [22] Leo Zhou, Sheng-Tao Wang, Soonwon Choi, H. Pichler, and M. D. Lukin, Quantum Approximate Optimization Algorithm: Performance, Mechanism, and Implementation on Near-Term Devices, *Phys. Rev. X* **10**, 021067 (2020).
- [23] J. R. Weggemans, A. Urech, A. Rausch, R. Spreeuw, R. Boucherie, F. Schreck, K. Schoutens, J. Minar, and F. Spielman, Solving correlation clustering with QAOA and a Rydberg qudit system: a full-stack approach, *Quantum* **6**, 687 (2022).
- [24] S. Ebadi, A. Keesling, M. Cain, T. T. Wang, H. Levine, D. Bluvstein, G. Semeghini, A. Omran, Jinguo Liu, R. Samajdar, Xiu-Zhe Luo, B. Nash, Xun Gao, B. Barak, E. Farhi, S. Sachdev, N. Gemelke, Leo Zhou, Soonwon Choi, H. Pichler, Shengtao Wang, M. Greiner, V. Vuletic, and M. D. Lukin, Quantum Optimization of Maximum Independent Set using Rydberg Atom Arrays, *Science* **376**, 1209 (2022).
- [25] D. Tiarks, S. Baur, K. Schneider, S. Dürr, and G. Rempe, Single-Photon Transistor Using a Förster Resonance, *Phys. Rev. Lett.* **113**, 053602 (2014).
- [26] H. Gorniaczyk, C. Tresp, J. Schmidt, H. Fedder, and S. Hofferberth, Single-Photon Transistor Mediated by Interstate Rydberg Interactions, *Phys. Rev. Lett.* **113**, 053601 (2014).
- [27] S. Baur, D. Tiarks, G. Rempe, and S. Dürr, Single-Photon Switch Based on Rydberg Blockade, *Phys. Rev. Lett.* **112**, 073901 (2014).
- [28] H. Gorniaczyk, C. Tresp, P. Bienias, A. Paris-Mandoki, W. Li, I. Mirgorodskiy, H. P. Büchler, I. Lesanovsky, and S. Hofferberth, Enhancement of Rydberg-mediated single-photon nonlinearities by electrically tuned Förster resonances, *Nat. Commun.* **7**, 12480 (2016).
- [29] W. Chen, K. M. Beck, R. Bückler, M. Gullans, M. D. Lukin, H. Tanji-Suzuki, and V. Vuletić, All-Optical Switch and Transistor Gated by One Stored Photon, *Science* **341**, 768 (2013).
- [30] T. G. Tiecke, J. D. Thompson, N. P. de Leon, L. R. Liu, V. Vuletić, and M. D. Lukin, Nanophotonic quantum phase switch with a single atom, *Nature (London)* **508**, 241 (2014).
- [31] Shuo Sun, Hyochul Kim, Zhouchen Luo, G. S. Solomon, and E. Waks, A single-photon switch and transistor enabled by a solid-state quantum memory, *Science* **361**, 57 (2018).
- [32] D. Aghamalyan, Jia-Bin You, Hong-Son Chu, Ching Eng Png, L. Krivitsky, and Leong Chuan Kwek, Tunable quantum switch realized with a single  $\Lambda$ -level atom coupled to the microtoroidal cavity, *Phys. Rev. A* **100**, 053851 (2019).
- [33] O. Kyriienko and A. S. Sørensen, Continuous-Wave Single-Photon Transistor Based on a Superconducting Circuit, *Phys. Rev. Lett.* **117**, 140503 (2016).
- [34] B. Royer, A. L. Grimsmo, A. Choquette-Poitevin, and A. Blais, Itinerant Microwave Photon Detector, *Phys. Rev. Lett.* **120**, 203602 (2018).
- [35] I. Iakoupov, Y. Matsuzaki, W. J. Munro, and S. Saito, Sequential nonabsorbing microwave single-photon detector, *Phys. Rev. Res.* **2**, 033238 (2020)
- [36] A. L. Grimsmo, B. Royer, J. M. Kreikebaum, Yufeng Ye, K. O'Brien, I. Siddiqi, and A. Blais, Quantum Metamaterial for Broadband Detection of Single Microwave Photons, *Phys. Rev. Applied* **15**, 034074 (2021).
- [37] Zhiling Wang, Zenghui Bao, Yan Li, Yukai Wu, Weizhou Cai, Weiting Wang, Xiyue Han, Jiahui Wang, Yipu Song, Luyan Sun, Hongyi Zhang, and Luming Duan, An ultra-high gain single-photon transistor in the microwave regime, *Nat. Commun.* **13**, 6104 (2022).
- [38] M. Fleischhauer, A. Imamoglu, and J. P. Marangos, Electromagnetically induced transparency: Optics in coherent media, *Rev. Mod. Phys.* **77**, 633 (2005).
- [39] K. Hammerer, A. S. Sørensen, and E. S. Polzik, Quantum interface between light and atomic ensembles, *Rev. Mod. Phys.* **82**, 1041 (2010).
- [40] E. Urban, T. A. Johnson, T. Henage, L. Isenhower, D. D. Yavuz, T. G. Walker, and M. Saffman, Observation of Rydberg blockade between two atoms, *Nat. Phys.* **5**, 110 (2009).
- [41] Hao, Y.M., Lin, G.W., Lin, X.M. et al. Single-photon transistor based on cavity electromagnetically induced transparency with Rydberg atomic ensemble, *Sci. Rep.* **9**, 4723 (2019).
- [42] A. A. Clerk, M. H. Devoret, S. M. Girvin, F. Marquardt, and R. J. Schoelkopf, Introduction to quantum noise, measurement, and amplification, *Rev. Mod. Phys.* **82**, 1155 (2010).
- [43] D. F. Walls and G. J. Milburn, *Quantum Optics* (Springer, 2nd edition, 2008).
- [44] D. Witthaut and A. S. Sørensen, Photon scattering by a three-level emitter in a one-dimensional waveguide, *New J. Phys.* **12**, 043052 (2010).
- [45] S. Fan, Ş. E. Kocabaş, and J.-T. Shen, Input-output formalism for few-photon transport in one-dimensional nanophotonic waveguides coupled to a qubit, *Phys. Rev. A* **82**, 063821 (2010).
- [46] The detailed procedure as well as full characterization of the system and several variations of the scheme are described in the accompanying Article.

- [47] J. Dalibard, Y. Castin, and K. Mølmer, Wave-function approach to dissipative processes in quantum optics, *Phys. Rev. Lett.* **68**, 580 (1992).
- [48] C. Gardiner and M. Collett, Input and output in damped quantum systems: Quantum stochastic differential equations and the master equation, *Phys. Rev. A* **31**, 3761 (1985).
- [49] K. Mølmer, Y. Castin, and J. Dalibard, Monte Carlo wave-function method in quantum optics, *J. Opt. Soc. Am. B* **10**, 524 (1993).
- [50] C. R. Murray, A. V. Gorshkov, and T. Pohl, Many-body decoherence dynamics and optimized operation of a single-photon switch, *New J. Phys.* **18**, 092001 (2016).
- [51] A. V. Gorshkov, A. André, M. D. Lukin, and A. S. Sørensen, Photon storage in  $\Lambda$ -type optically dense atomic media. I. Cavity model, *Phys. Rev. A* **76**, 033804 (2007).
- [52] A. V. Gorshkov, A. André, M. D. Lukin, and A. S. Sørensen, Photon storage in  $\Lambda$ -type optically dense atomic media. II. Free-space model, *Phys. Rev. A* **76**, 033805 (2007).
- [53] E. Zeuthen, M. J. Gullans, M. F. Maghrebi, and A. Gorshkov, Correlated Photon Dynamics in Dissipative Rydberg Media, *Phys. Rev. Lett.* **117**, 043602 (2017).
- [54] D. Pinotsi and A. Imamoglu, Single Photon Absorption by a Single Quantum Emitter, *Phys. Rev. Lett.* **100**, 093603 (2008).
- [55] J. Vaneeckloo, S. Garcia and A. Ourjoumtsev, Intracavity Rydberg Superatom for Optical Quantum Engineering: Coherent Control, Single-Shot Detection, and Optical  $\pi$  Phase Shift, *Phys. Rev. X* **12**, 021034 (2022).
- [56] T. Stolz, H. Hegels, M. Winter, B. Röhr, Y. Hsiao, L. Husel, G. Rempe and S. Dürr, Quantum-Logic Gate between Two Optical Photons with an Average Efficiency above 40%, *Phys. Rev. X* **12**, 021035 (2022).